

Time-varying signal analysis to detect high-altitude periodic breathing in climbers ascending to extreme altitude

**A. Garde, B. F. Giraldo, R. Jané,
T. D. Latshang, A. J. Turk, T. Hess,
M. M. Bosch, D. Barthelmes, T. M. Merz,
J. Pichler Hefti, et al.**

Medical & Biological Engineering & Computing

ISSN 0140-0118

Med Biol Eng Comput
DOI 10.1007/s11517-015-1275-x



Your article is protected by copyright and all rights are held exclusively by International Federation for Medical and Biological Engineering. This e-offprint is for personal use only and shall not be self-archived in electronic repositories. If you wish to self-archive your article, please use the accepted manuscript version for posting on your own website. You may further deposit the accepted manuscript version in any repository, provided it is only made publicly available 12 months after official publication or later and provided acknowledgement is given to the original source of publication and a link is inserted to the published article on Springer's website. The link must be accompanied by the following text: "The final publication is available at link.springer.com".

Time-varying signal analysis to detect high-altitude periodic breathing in climbers ascending to extreme altitude

A. Garde¹ · B. F. Giraldo¹ · R. Jané¹ · T. D. Latshang² · A. J. Turk³ · T. Hess⁴ ·
M. M. Bosch⁵ · D. Barthelmes⁵ · T. M. Merz⁶ · J. Pichler Hefti⁷ · O. D. Schoch⁸ ·
K. E. Bloch²

Received: 29 October 2013 / Accepted: 3 March 2015
© International Federation for Medical and Biological Engineering 2015

Abstract This work investigates the performance of cardiorespiratory analysis detecting periodic breathing (PB) in chest wall recordings in mountaineers climbing to extreme altitude. The breathing patterns of 34 mountaineers were monitored unobtrusively by inductance plethysmography, ECG and pulse oximetry using a portable recorder during climbs at altitudes between 4497 and 7546 m on Mt. Muztagh Ata. The minute ventilation (V_E) and heart rate (HR) signals were studied, to identify visually scored PB, applying time-varying spectral, coherence and entropy analysis. In 411 climbing periods, 30–120 min in duration, high values of mean power (MP^{VE}) and slope ($MSlope^{VE}$) of the modulation frequency band of V_E , accurately identified PB, with an area under the ROC curve of 88 and 89 %, respectively. Prolonged stay at altitude was associated with an increase in PB. During PB episodes, higher peak power of ventilatory (MP^{VE}) and cardiac (MP_{LF}^{HR}) oscillations and

cardiorespiratory coherence (MP_{LF}^{Coher}), but reduced ventilation entropy ($SampEn^{VE}$), was observed. Therefore, the characterization of cardiorespiratory dynamics by the analysis of V_E and HR signals accurately identifies PB and effects of altitude acclimatization, providing promising tools for investigating physiologic effects of environmental exposures and diseases.

Keywords High-altitude periodic breathing · Cardiorespiratory characterization · Time-varying spectral analysis · Acclimatization · Hypoxia

1 Introduction

High-altitude periodic breathing (PB) is a pattern of waxing and waning of ventilation observed in healthy subjects

✉ A. Garde
ainara.garde@upc.edu
B. F. Giraldo
beatriz.giraldo@upc.edu
R. Jané
raimon.jane@upc.edu
K. E. Bloch
konrad.bloch@usz.ch

¹ Biomedical Signal Processing and Interpretation (BIOSPIN) Group, Department of ESAT, Institut de Bioenginyeria de Catalunya (IBEC) and CIBER de Bioingeniería, Biomateriales y Nanomedicina (CIBER-BBN), Universitat Politècnica de Catalunya (UPC), C/Baldiri Reixac, 4, 08028 Barcelona, Spain

² Pulmonary Division, University Hospital of Zurich, Zurich, Switzerland

³ High Altitude Clinic Wald, Wald, Switzerland

⁴ Pulmonary Division, Cantonal Hospital Winterthur, Winterthur, Switzerland

⁵ Department of Ophthalmology, University Hospital Zurich, Zurich, Switzerland

⁶ Intensive Care Unit, University Hospital of Berne, Berne, Switzerland

⁷ Pulmonary Division, University Hospital of Berne, Berne, Switzerland

⁸ Pulmonary Division, Cantonal Hospital St. Gallen, St. Gallen, Switzerland

exposed to hypobaric hypoxia [4, 28]. It shares pathophysiologic aspects with the central sleep apnea syndrome and with Cheyne–Stokes respiration in patients with heart failure [5, 10]. Thus, the hyperventilation observed in both subjects exposed to high altitude as well as in certain patients with heart failure reflects an increase in ventilatory drive. While this mitigates hypoxemia and thereby contributes to improved arterial oxygen transport, it is associated with hypocapnia [37]. This results in a decrease in the CO₂ reserve, which is the difference between the arterial carbon dioxide partial pressure (PaCO₂) during stable breathing (eupnea) and the apnea threshold, the PaCO₂ below which the drive to breathe ceases and central apnea ensues [10, 21]. In conditions with high ventilatory sensitivity to CO₂ such as in subjects exposed to high altitude or in heart failure patients, central apneas are followed by an overshooting period of hyperventilation resulting again in hypocapnia, which perpetuates periodic ventilatory oscillations. PB may disrupt sleep and be perceived as intermittent dyspnea. Therefore, sleep at high altitude is often perceived as fragmented and less restorative compared with lowlands [38].

Related to differences in the feed-back control system (plant and controller gain, circulation time [20]) the cycle length of periodic breathing is shorter in healthy subjects exposed to hypobaric hypoxia (i.e., in the order of 15–25 s [4]), compared with patients with Cheyne–Stokes respiration due to heart failure (i.e., 25–100 s [6]). Ventilatory

control instability causes changes in the cardiac autonomic regulation, which can be evaluated by analysis of heart rate variability (HRV) [35].

PB has been thought to occur predominantly or exclusively at rest and during sleep when the wakefulness drive to breathe is reduced and ventilation is controlled by autonomic chemical feed-back control [11]. However, detection of PB during exercise has been hampered by technical and physiologic limitations. For example, a poor signal-to-noise ratio of respiratory signals during physical activity, damping effects of added external dead space associated with measurements [1] and cortical influences overriding autonomic rhythms may all impair the identification of PB. In addition to these limitations, visual detection of PB is tedious and time consuming. Therefore, computerized signal analysis is promising to quantify periodic oscillations in cardiac and respiratory signals although the optimal technique has not been established.

Accordingly, in this study, we aimed to evaluate the performance of several time-varying signal processing approaches for detection of PB comparing them with visual reference of PB, scored by an expert clinician based on guidelines to measure breathing disorders [33]. We analyzed data recorded in mountaineers participating in a medical research expedition to Mount Muztagh Ata, 7546 m, China [3, 4, 23]. Ventilation was continuously recorded through unobtrusive chest wall recordings using portable

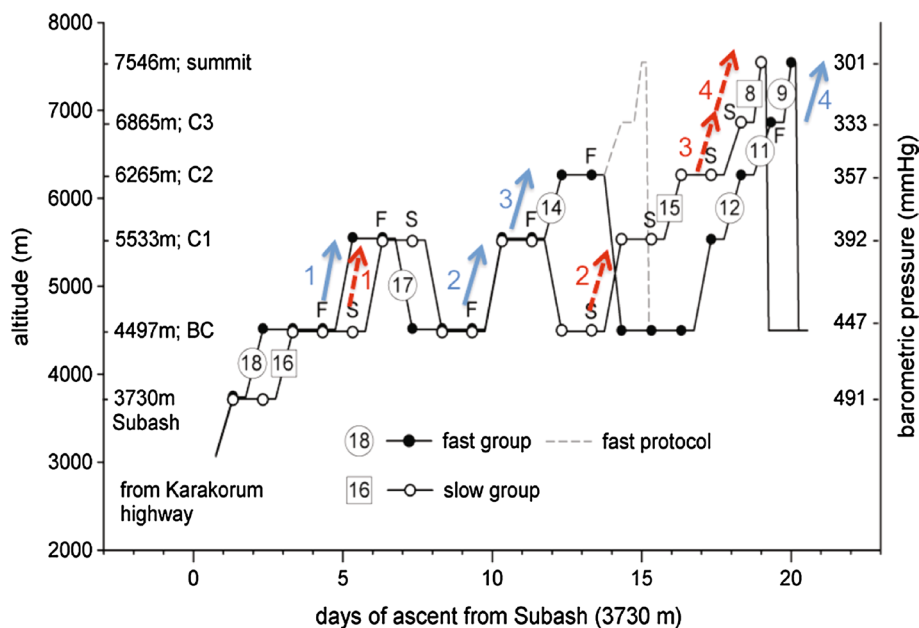


Fig. 1 Protocol of the expedition from Subash (3730 m), via base camp (BC) and high camps (C1, C2, C3) to the summit (7546 m). Two groups of 18 and 16 mountaineers, ascended with different protocols. Closed and open circles represent overnight stays of the fast and slow groups, respectively, in a camp. The number of subjects in each group ascending to and beyond a certain point is indicated

within circles (fast group, solid circles) and rectangles (slow group, open circles) on the lines representing the corresponding ascent. The solid and dotted arrows indicate daytime ascents of the fast and slow groups analyzed in this study, respectively (edited from [4] Copyright© 2010 by American Journal of Respiratory and Critical Care Medicine. Reprinted by permission of American Thoracic Society)

inductive plethysmography while mountaineers climbed from very high to extreme altitude [13] (from 4497 m up to 7546 m, Fig. 1). We hypothesized that time-varying signal processing techniques applied to minute ventilation (V_E) and heart rate (HR) signals accurately quantify PB and allow identification of physiologic adaptation to varying degrees of hypoxia at altitude. The findings gained by these studies may help to better comprehend the mechanisms of diseases associated with hypoxia and give valuable insights into mechanisms and therapeutic targets in other disorders of ventilatory control.

2 Materials and methods

2.1 Subjects, measurements and protocol

The study was performed as part of a medical research expedition to Mount Muztagh Ata (7546 m, China) [3, 4, 22]. The protocol was approved by the ethics committee of the Zurich University, subjects gave written informed consent, and the study is registered at ClinicalTrials.gov NTC00603122. As previously described in detail, 34 healthy mountaineers (median age 46 years, range 26–65 years) climbed from the Muztagh Ata base camp (BC) at 4497 m via three high camps (C1, C2, C3) to the summit at 7546 m, within 19–20 days (Fig. 1) [3]. Physiologic recordings were continuously obtained during climbs in the field by a portable device of the size of a palmtop computer (LifeShirt, VivoMetrics, CA, USA). It incorporated pulse oximetry, electrocardiography (ECG), accelerometers and calibrated respiratory inductive plethysmography as previously described [4]. With this unobtrusive technique, ventilation is monitored through chest wall sensors without the need for airway instrumentation. We have extensively validated the accuracy of ventilation measured by this technique [1, 9]. The barometric pressure was continuously recorded by wrist sensors to track the altitude and hypoxia exposure of the climbers [27].

2.2 Visual analysis of recordings

Data stored in the LifeShirt monitoring devices were downloaded into a personal computer and signals displayed on the video screen using specialized software (VivoLogic V2.1, VivoMetrics, Loma Linda, CA, USA). An investigator experienced with breathing pattern analysis (Konrad E. Bloch) reviewed recordings from each climb lasting for 6–9 h in a day. Four periods of continuous climbing, lasting 30–120 min each, were identified based on climber's log books, altimeter and accelerometer signals, and visual inspection of inductance, ECG and pulse oximeter signals. In the selected recordings that were free of major artifacts,

PB cycles were scored visually and manually labeled. According to previously reported guidelines [35], PB was visually identified based on the inductive plethysmographic sum volume signal if there was a waxing and waning of breathing amplitude for at least three cycles, with transient reductions in amplitude to <50 % of the previous 2-min baseline for >5 s, interrupted by periods of hyperventilation [4]. According to visual scoring, a total of 411 periods from various altitudes (from 4497 m up to 7546 m) were available for analysis, 40 with PB and 371 without PB (nPB). The periodic breathing index (PBI), defined as the number of periodic breathing cycles per hour, and the oxygen desaturation index, defined as the mean number of desaturations (≥ 4 % dips) from baseline per hour, were computed. The mean oxygen saturation by pulse oximetry (SpO_2) and the altitude range for each climbing period were also recorded. The data were further processed by the techniques described below.

2.3 Computer-assisted time series analysis

The time-varying cardiorespiratory analysis to detect high-altitude PB involved the following steps: preprocessing signals, time-varying power spectral analysis, coherence and complexity analysis (approximate and sample entropy), and selection of relevant variables for identification and quantification of PB. These analyses were performed using MATLAB version 7.13 (R2011b). Details are provided in the "Appendix."

2.3.1 Preprocessing

Respiratory inductance plethysmography signals, recorded at a sample frequency of 50 Hz, were calibrated by the qualitative diagnostic calibration method, during natural breathing [31], followed by a fixed volume calibration using rebreathing into a bag of known volume (0.8 L) at the beginning and end of each climb as described previously [7]. Accuracy of calibration was previously verified and was regarded as acceptable if inductive plethysmographic tidal volumes were within 20 % of calibration bag volume. Thus, recordings in which tidal volume calibration at the beginning deviated by more than 20 % from that at the end were discarded. Time series of breath-by-breath minute ventilation (V_E) and heart rate (HR) were selected as the most appropriate signals for this study because they are essential for pulmonary and circulatory gas transport. V_E was computed by multiplying the inspiratory tidal volume by the inspiratory rate, both measured in every respiratory cycle. The inspiratory tidal volume corresponds to the amplitude of the volume signal extracted from every breath cycle. V_E calculated breath by breath was interpolated to 1 Hz using a cubic spline function.

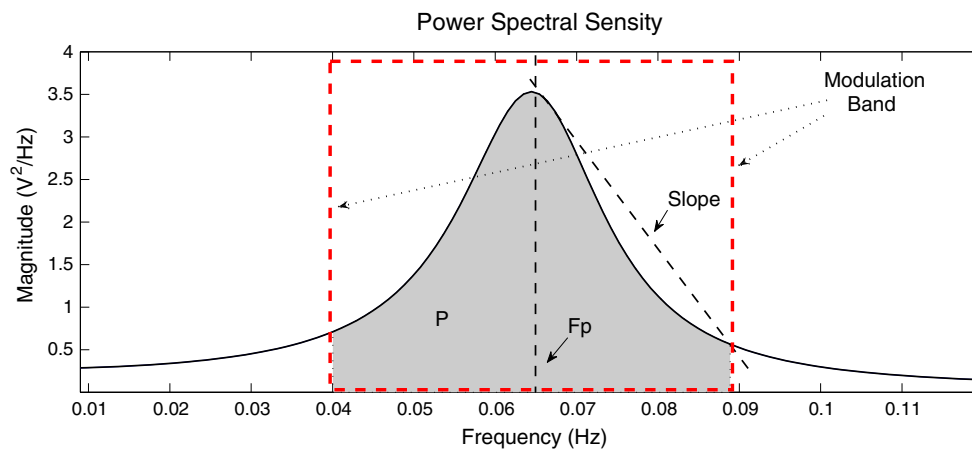


Fig. 2 Illustration of variables derived from time series analysis. PSD is extracted for a time window, and the following parameters are extracted from the modulation frequency band. F_p modulation fre-

quency peak, P power within the modulation frequency band, *Slope* slope from F_p to the high end of the modulation band

RR time series were extracted from the ECG sampled at 1000 Hz. The RR time intervals that exceed three times the standard deviation of mean RR were removed recursively to reduce the artifact influence. The sequence of instantaneous heart rates, reciprocal to RR time series, is analyzed in this study [25]. Heart rate (HR) signal was obtained by interpolating the inverse of RR time series to 1 Hz using a cubic spline function. Both V_E and HR signals were normalized to unity, and their baseline was removed through a zero-phase second-order high-pass filter. Previous studies have shown that the cycle time of high-altitude periodic breathing may be as short as 15 s [4]. Therefore, a cutoff frequency of 0.008 Hz was found appropriate to filter the baseline.

2.3.2 Time-varying signal processing techniques

Often the same subject during rest and during physical activities of various types and intensities presents a mixture of breathing patterns, ranging from breathing without cyclic modulation through mild PB to more severe PB superimposed on nonperiodic variations in ventilation related to physical and emotional activities, speech and other stimuli. Conventional spectral analysis assumes a stationary signal and is therefore unable to identify pattern changes. An approach to account for such changes is to implement a time-varying spectral and coherence analysis [14, 36]. Using a 6-min sliding time window with 75 % overlap, both V_E and HR signals are divided into segments assumed to be stationary and suitable for power spectral density (PSD) and coherence analysis.

The PSD obtained for each time window was characterized through the following variables: (1) the modulation frequency peak (F_p), defined as the maximum value within

the frequency band ranging from 0.01 to 0.4 Hz, (2) the power (P) within the modulation frequency band, defined as a fixed frequency band of 0.1 Hz centered at the modulation frequency peak and (3) the slope between modulation frequency peak and the right end of the modulation frequency band as illustrated in Fig. 2.

According to published guidelines [25], the analysis of the HR time series was focused on three main frequency bands: very low frequency range (VLF, $f < 0.04$ Hz), low frequency range (LF, $0.04 \text{ Hz} < f < 0.15$ Hz) and high frequency range (HF, $0.15 \text{ Hz} < f < 0.4$ Hz). The distribution of the power of LF and HF may vary in relation to changes in autonomic modulations of HR. The time-varying normalized power of VLF, LF and HF bands was evaluated. The cardiorespiratory interaction was evaluated in terms of the normalized power of the coherence between V_E and HR in VLF, LF and HF bands. Furthermore, complexity analysis based on sample and approximate entropy was applied to both V_E and HR signals. This approach allowed us to determine a single number that reflects the randomness (complexity) of the cardiorespiratory pattern. According to Pincus [29], we worked with $m = 2$ and $r = 0.15$ because this was the lowest tolerance value that presented differences between periods with and without PB. Further details are provided in Fig. 7 in “Appendix.”

2.4 Selection of variables and evaluation of diagnostic performance

Table 1 describes the variables used to characterize the breathing pattern, heart rate variability and their interaction. Evaluation of diagnostic performance of variables derived from signal processing versus visual scores of PB was performed by linear discriminant analysis and receiver

Table 1 Variables derived from statistical signal processing (see Fig. 2)

Analysis	Abbreviation	Definition	Description
Breathing pattern	$MP^{VE} (V^2)$	Mean power of modulation band	Captures the strength of periodicity in ventilation
	$MFp^{VE} (Hz)$	Mean of modulation frequency peak	Captures the modulation frequency
	$MSlope^{VE} (V^2/Hz)$	Mean slope between modulation frequency peak and end of the modulation frequency band	Reflects strength of periodicity in ventilation, i.e., the “sharpness” of the peak
	$SDMP^{VE} (V^2)$	Standard deviation of the power of the modulation band	Evaluates the stationarity of the periodicity in ventilation
	$SDMSlope^{VE} (V^2/Hz)$	Standard deviation of the slope between modulation frequency peak and higher end of the modulation band	Evaluates the stationarity of the sharpness of the peak
	$SDMFp^{VE} (Hz)$	The standard deviation of the modulation frequency peak	Evaluates the stationarity of the modulation frequency peak
Heart rate variability	$MP_{VLF}^{HR} (nu)$	The mean cardiac power at very low frequency range (<0.04 Hz)	Quantifies heart rate variability in different frequency ranges
	$MP_{LF}^{HR} (nu)$	The mean cardiac power at low frequency range (0.04–0.15 Hz)	
	$MP_{HF}^{HR} (nu)$	The mean cardiac power at high frequency range (0.15–0.4 Hz)	
	$M_{HR} (Hz)$	The mean of heart rate	Quantifies heart rate
	$SDM_{HR} (Hz)$	The standard deviation of heart rate	
Cardiorespiratory complexity	$SampEn^{VE}$	Sample entropy applied to minute ventilation	Quantifies complexity in ventilation
	$ApEn^{VE}$	Approximate entropy applied to minute ventilation	
	$SampEn^{HR}$	Sample entropy applied to heart rate	Quantifies complexity in heart rate
Cardiorespiratory interaction	$ApEn^{HR}$	Approximate entropy applied to heart rate	
	$MP_{VLF}^{Coher} (nu)$	The mean power of the coherence between V_E and HR at very low frequency range (<0.04 Hz)	Quantifies cardiorespiratory interaction in different frequency ranges
	$MP_{LF}^{Coher} (nu)$	The mean power of the coherence between V_E and HR at low frequency range (0.04–0.15 Hz)	
	$MP_{HF}^{Coher} (nu)$	The mean power of the coherence between V_E and HR at high frequency range (0.15–0.4 Hz)	

operating characteristic (ROC) analysis. Altitude acclimatization is a time-dependent process of physiologic adaption to hypoxic conditions at altitude. The effect of acclimatization on variables derived from signal processing was assessed by comparing data from climbs over the same route (climb from BC, 4497 m to C1, 5533 m) within 5–8 days (Fig. 1).

2.4.1 Statistics

Statistical analysis was performed using IBM SPSS Statistics software (v 19). Data are summarized as medians (first and third quartiles) to account for nonnormal data distribution. Differences were evaluated by Mann–Whitney *U* test. A probability of $p < 0.05$ was considered significant,

applying a Bonferroni correction where appropriate. A parameter selection process was implemented over the statistically significant parameters using linear discriminant analysis. Leave-one-out cross-validation technique was applied to the limited number of climbing periods.

3 Results

Figures 3 and 4 show the time-varying PSD of V_E and HR signals and their coherence for a mountaineer with and without PB, respectively. The most striking feature in these diagrams is the temporal evolution of the modulation frequency peak in both spectra, and the high coherence in low frequency band presented by the subject with PB.

Fig. 3 **a** 6-min segment of minute ventilation (V_E), **b** 6-min segment of heart rate (HR), **c** PSD applied to 6-min V_E , **d** PSD applied to 6-min HR, **e** V_E with the 6-min sliding window represented in *black*, **f** HR with the 6-min sliding window represented in *black*, **g** time-varying PSD applied to V_E , **h** time-varying PSD applied to HR and **i** time-varying coherence between V_E and HR, of a subject with PB

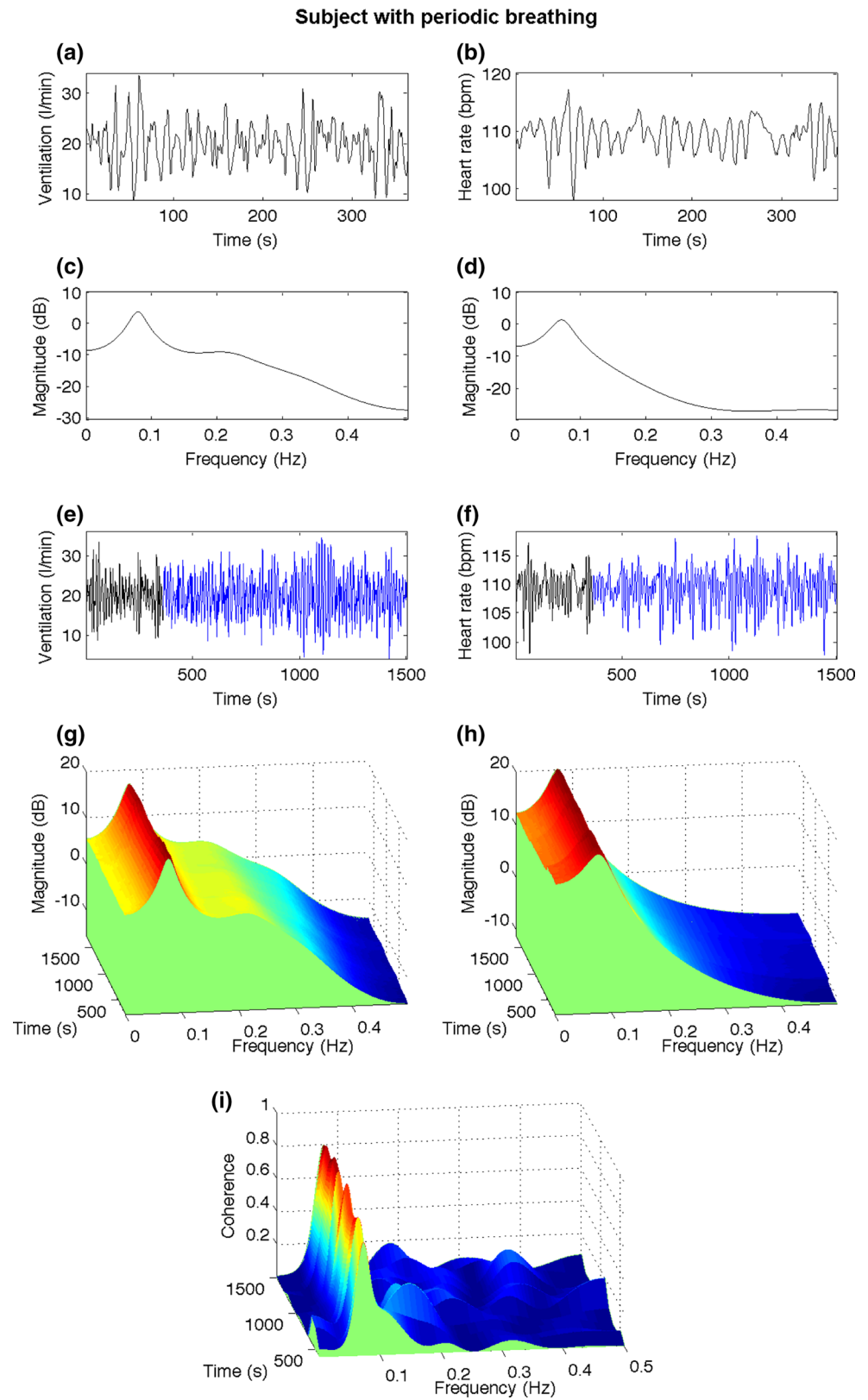
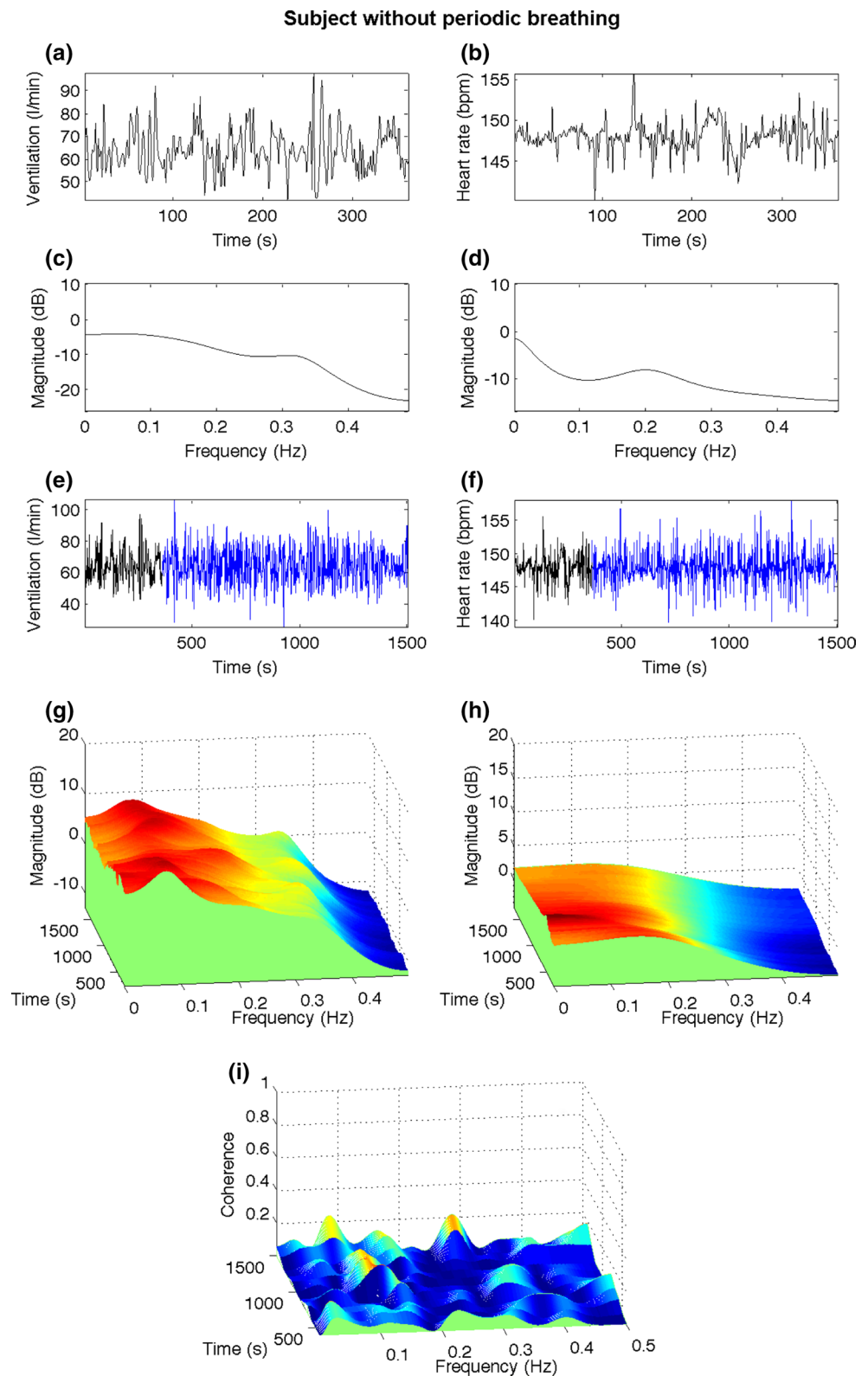


Fig. 4 **a** 6-min segment of minute ventilation (V_E), **b** 6-min segment of heart rate (HR), **c** PSD applied to 6-min V_E , **d** PSD applied to 6-min HR, **e** V_E with the 6-min sliding window represented in *black*, **f** HR with the 6-min sliding window represented in *black*, **g** time-varying PSD applied to V_E , **h** time-varying PSD applied to HR and **i** time-varying coherence between V_E and HR, of a subject without PB



3.1 Classification of recordings with and without PB

The accuracy of statistical signal processing techniques in classification between 40 PB and 371 nPB periods was

evaluated in a first step by comparing mean values between the two sets of data (Table 2). Both, the mean of the power (MP^{VE}) and the slope ($MSlope^{VE}$) of the modulation frequency band are significantly higher in PB climbing periods

Table 2 Results of time-varying signal processing

	Recording periods with periodic breathing (PB)	Recording periods without periodic breathing (nPB)	<i>p</i> value
MP ^{VE}	0.78 (0.72, 0.84)	0.53 (0.47, 0.61)	≤0.0005
MFp ^{VE}	0.069 (0.06, 0.07)	0.074 (0.07, 0.09)	0.02
MSlope ^{VE}	0.55 (0.36, 0.77)	0.12 (0.08, 0.20)	≤0.0005
SDMP ^{VE}	0.04 (0.03, 0.05)	0.06 (0.04, 0.08)	≤0.0005
SDMFp ^{VE}	0.003 (0.002, 0.005)	0.02 (0.006, 0.03)	≤0.0005
SDMSlope ^{VE}	0.19 (0.1, 0.3)	0.07 (0.04, 0.13)	≤0.0005
MP ^{HR} _{VLF}	0.25 (0.21, 0.34)	0.44 (0.34, 0.53)	≤0.0005
MP ^{HR} _{LF}	0.67 (0.57, 0.75)	0.41 (0.34, 0.53)	≤0.0005
MP ^{HR} _{HF}	0.05 (0.03, 0.07)	0.07 (0.04, 0.12)	0.01
M _{HR}	1.08 (1.43, 2.04)	1.98 (1.84, 2.11)	0.002
ApEn ^{VE}	1.51 (1.39, 1.70)	1.66 (1.51, 1.74)	0.02
SampEn ^{VE}	1.47 (1.30, 1.77)	1.76 (1.54, 1.97)	0.0002
ApEn ^{HR}	1.31 (1.06, 1.64)	1.51 (1.34, 1.64)	0.03
SampEn ^{HR}	1.25 (0.90, 1.63)	1.50 (1.31, 1.70)	0.007
MP ^{Coher} _{VLF}	0.08 (0.06, 0.1)	0.10 (0.08, 0.13)	0.0003
MP ^{Coher} _{LF}	0.53 (0.45, 0.60)	0.35 (0.29, 0.43)	≤0.0005
MP ^{Coher} _{HF}	0.30 (0.26, 0.38)	0.42 (0.35, 0.49)	≤0.0005

Values are medians (quartiles). Analysis includes 40 periods with and 371 periods without periodic breathing. Abbreviation and units (Table 1)

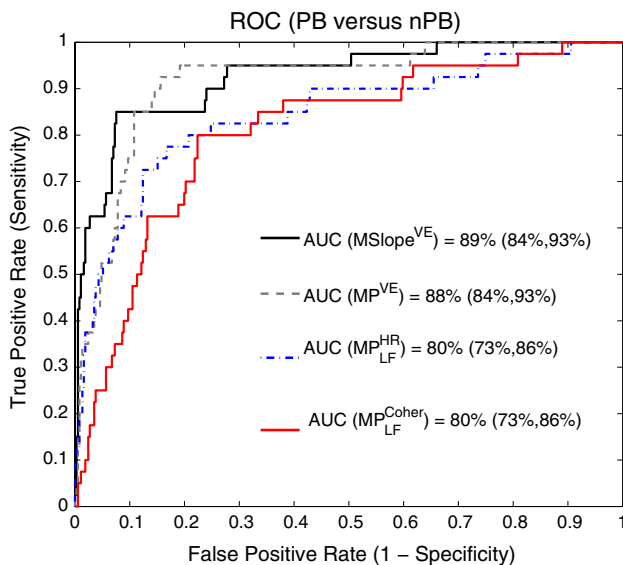


Fig. 5 ROC curves classifying PB versus nPB, obtained with the most significant parameters (MP^{HR}_{LF}, MP^{VE}, MSlope^{VE} and MP^{Coher}_{LF}), see Table 2. The numbers for the area under the ROC curve and the corresponding 95 % confidence interval (in brackets) are inserted into figure

than in nPB periods. The mean of cardiac power and coherence between V_E and HR on the low frequency band (MP^{HR}_{LF} and MP^{Coher}_{LF}, respectively) are significantly higher in PB climbing periods. Cardiac (SampEn^{HR}, ApEn^{HR}) and ventilatory complexities (SampEn^{VE}, ApEn^{VE}) are decreased in

PB compared with nPB periods. Figure 5 presents the ROC curve obtained with the most discriminative variables.

Including data from all (from BC at 4497 m to the summit at 7546 m), correlation analysis between several variables derived from signal processing was performed. This revealed significant positive correlations ($r > 0.5$, p value < 0.0005) between the variables derived from the ventilation signal (MP^{VE} and MSlope^{VE}) as well as with low-frequency cardiac power (MP^{HR}_{LF}) and cardiorespiratory coherence (MP^{Coher}_{LF}). In contrast, significant negative correlations were found between variables derived from spectral analysis of the ventilation and HR signals with entropy measures. MP^{VE}, for example, presents a negative correlation of $r = -0.7$, p value < 0.0005 with both ventilation entropy measures (SampEn^{VE} and ApEn^{VE}) and $r = -0.5$, p value < 0.0005 , with HR, reflecting lower ventilation complexity and lower cardiac rate (M^{HR}) during PB. Figure 6 illustrates some of these results. In addition, positive weakly-to-moderately significant correlations ($r = 0.3$ and $r = 0.5$) were found between the approximate and sample entropy of the HR signal (SampEn^{HR} and ApEn^{HR}) and high-frequency cardiac power (MP^{HR}_{HF}), suggesting that higher HR complexity is associated with higher cardiac power at the high frequency band.

SpO₂ decreased at higher altitudes, reflected by a negative correlation ($r < -0.5$, p value < 0.0005) as expected, and low SpO₂ values were found to be associated with higher HR values (M_{HR}) ($r < -0.3$, p value < 0.001).

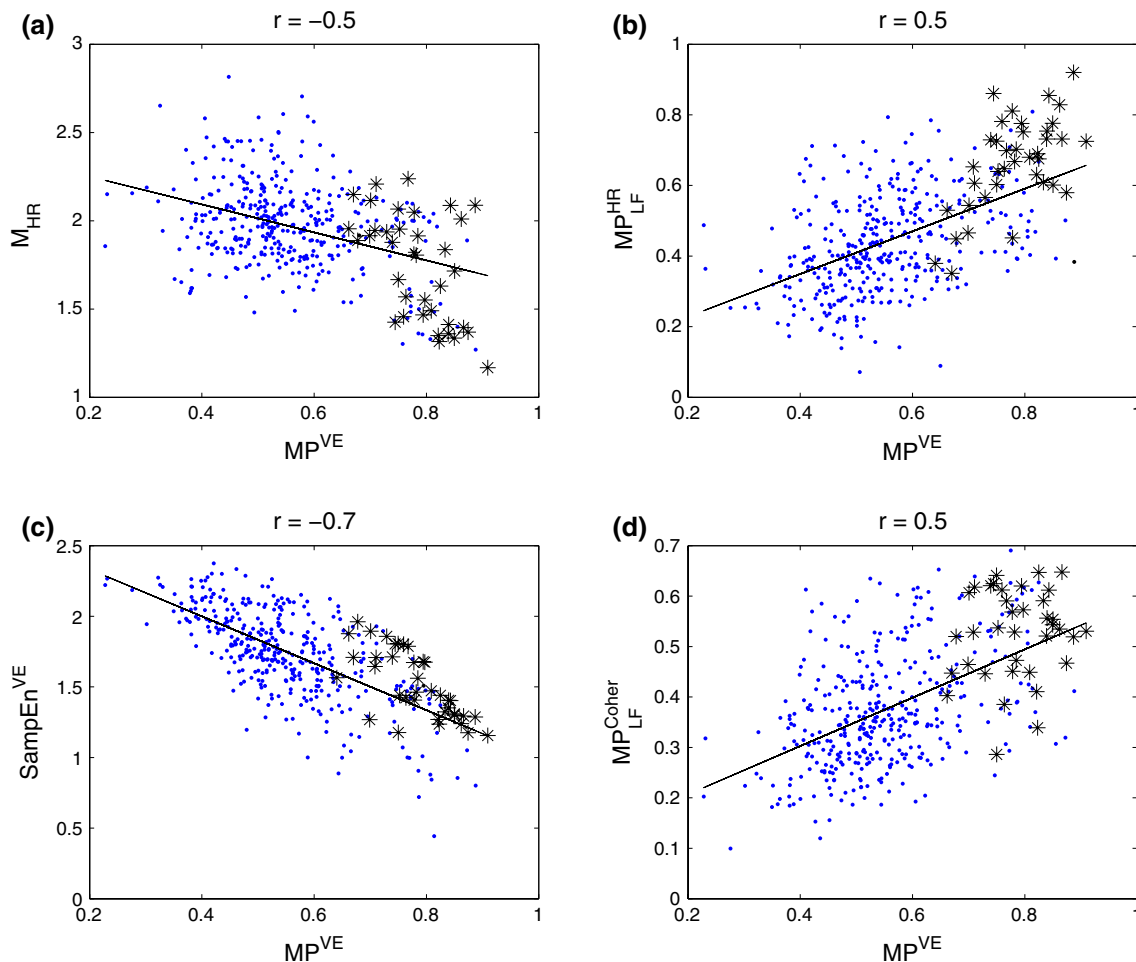


Fig. 6 Correlations between **a** MP^{VE} and M_{HR} , **b** MP^{VE} and MP_{LF}^{HR} , **c** MP^{VE} and $SampEn^{VE}$ and **d** MP^{VE} and MP_{LF}^{Coher} , where PB periods are represented by stars and nPB periods by dots

Table 3 Effects of acclimatization (from 4497 to 5533 m) quantified by variables from signal processing

	First ascent days 5 (fast) and 6 (slow)	Second ascent days 10 (fast) and 14 (slow)	<i>p</i> value
MP^{VE}	0.54 (0.48, 0.63)	0.58 (0.51, 0.65)	0.05
$MSlope^{VE}$	0.12 (0.08, 0.2)	0.15 (0.10, 0.25)	0.02
MP_{VLF}^{HR}	0.45 (0.30, 0.55)	0.37 (0.28, 0.46)	0.007
MP_{LF}^{HR}	0.39 (0.31, 0.47)	0.50 (0.40, 0.62)	<0.0005
MP_{HF}^{HR}	0.08 (0.05, 0.19)	0.06 (0.05, 0.11)	0.006
M_{HR}	1.86 (1.72, 2.00)	2.05 (1.89, 2.19)	<0.0005
SDM_{HR}	0.081 (0.062, 0.10)	0.066 (0.054, 0.083)	<0.0005
$SampEn^{HR}$	1.62 (1.42, 1.79)	1.50 (1.31, 1.70)	0.005
$ApEn^{HR}$	1.60 (1.43, 1.68)	1.51 (1.37, 1.65)	0.003
MP_{LF}^{Coher}	0.34 (0.27, 0.43)	0.36 (0.30, 0.47)	0.02
SpO_2	73 (69, 76)	77 (74, 81)	<0.002
PBI^a	PB: 11 (8, 17)	PB: 19 (9, 33)	0.02

Values are medians (quartiles). Analysis includes 11 periods with and 119 without PB in the first ascent, and 17 periods with and 110 without PB in the second ascent

^a *PBI* reflects the number of periodic breathing cycles per hour, and PB reflects the number of ascending periods classified as periodic breathing by the expert. Abbreviations and units (Table 1)

3.2 Effect of acclimatization

As Fig. 1 illustrates, the subjects climbed the same ascent from BC (4497 m) to C1 (5533 m) twice within a few days allowing assessment of acclimatization effects. Table 3 shows variables derived from the first and the second ascent, climbing from 4497 to 5533 m. We have 130 (11 PB, 119 nPB) periods in the first ascent and 127 (17 PB, 110 nPB) periods in the second ascent. It can be observed that both SpO_2 and PBI increase with acclimatization while HR decreases. Certain spectral parameters that reflect PB, such as MP^{VE} , $\text{MSlope}^{\text{VE}}$, $\text{MP}_{\text{LF}}^{\text{HR}}$ and $\text{MP}_{\text{LF}}^{\text{Coher}}$, increase from first to second ascent (Table 3).

4 Discussion

In this study, we have proposed the characterization of cardiorespiratory dynamics using the minute ventilation signal and heart rate signal to automatically detect and quantify high-altitude periodic breathing (PB). Based on a unique set of cardiorespiratory recordings obtained unobtrusively in 34 mountaineers climbing to extreme altitude and reference PB scores, we found that variables derived from time-varying analysis of spectral density, entropy and coherence performed accurately in identifying and quantifying high-altitude PB and effects of acclimatization. These promising results allow an objective evaluation of the effect of hypobaric hypoxia on control of breathing even in conditions of low signal-to-noise ratio and will provide a powerful alternative to tedious and time-consuming visual assessment.

Spectral characterization of the envelope of the respiratory flow signal, acquired at rest using a pneumotachograph, was successfully applied to identify PB and Cheyne–Stokes respiration in heart failure patients [15]. These results improved by applying a nonlinear spectral characterization to the respiratory flow signal through the innovative correntropy function [16]. In that database, the respiratory flow signal of heart failure patients at rest was acquired using a pneumotachograph. Conversely, in the current study the volume signal was derived from chest wall recordings without airway instrumentation. The respiratory pattern characterization through the analysis of the respiratory volume signal was performed previously to detect and quantify high-altitude periodic breathing (PB) [18]. Higher power of the modulation frequency band detected by parametric spectral analysis and higher respiratory frequencies were observed at lower SpO_2 . In the current study, we extend the application of parametric power spectral analysis to the minute ventilation and heart rate signal obtained unobtrusively in subjects during physical activities of variable intensity and under harsh environmental conditions at extreme altitude.

We evaluated the discrimination of recordings with and without periodic breathing by several variables derived from the spectral analysis, cardiorespiratory coherence and entropy of the time series of ventilation and HR. Although several variables were significantly correlated among each other (Fig. 6), we found that the power (MP^{VE}) and slope ($\text{MSlope}^{\text{VE}}$) of the ventilation modulation frequency band performed particularly well in identifying visually scored PB and nPB periods correctly, i.e., in 88 and 89 % of instances, respectively (Fig. 5). The accurate identification of PB recordings through the characterization of cardiorespiratory dynamics suggests that this approach is promising and that these variables could be valuable indices to quantify and evaluate PB by computer-assisted automatic analysis.

In terms of physiologic adaptation, it is remarkable that PB was observed by visual analysis and identified by time-varying signal processing of ventilation and HR, along all the ascents even during heavy physical exertion. Enhanced spectral power in both V_E and HR signals (MP^{VE} , $\text{MP}_{\text{LF}}^{\text{HR}}$) and higher cardiorespiratory interaction ($\text{MP}_{\text{LF}}^{\text{Coher}}$) were identified in the low frequency band, which coincides with the periodic breathing oscillations frequency range. Ventilation instability is therefore clearly interacting with heart rate. Previous research on the analysis of HRV in response to PB in patients with congestive heart failure revealed a high power at VLF [26, 35]. Conversely, in the healthy mountaineers exposed to hypobaric hypoxia in the current study we observed a high power in the LF band. These differences are consistent with the longer cycle times of PB in heart failure patients compared with those of healthy subjects [12]. These results coincide with the findings reported by Lipsitz et al. [24] showing high cardiac power at LF due to high-altitude PB.

Regarding the complexity analysis, cardiac and ventilatory entropy decreased significantly in periods with PB, reflecting lower cardiorespiratory complexity during PB associated with exposure to hypobaric hypoxia. Decreases in entropy of cardiac interbeat intervals have also been observed in conditions of cardiovascular stress associated with heart failure [16, 30] at rest, and even in heart failure patients performing their usual daytime activities [6].

Different physiologic conditions seem to have different complexity and regularity properties. Thus, we employed not only spectral analysis but evaluated entropy within physiologic signals of mountaineers as well. The presence of PB was negatively correlated with variables reflecting cardiorespiratory entropy (Fig. 6). Therefore, periodic breathing seems to reduce complexity within the variability of ventilation and HR. The reduced complexity within the corresponding physiologic signals in heart failure patients with breathing disorders and higher risk condition is consistent with the notion that entropy measures are negatively

correlated with conditions of physiologic stress such as hypoxia or heart failure [17].

The effect of acclimatization could be assessed by comparing data from subjects climbing the same ascent twice within a few days (Fig. 1). Acclimatization is associated with a number of physiologic adjustments including an increased ventilatory drive. It increases ventilation and mitigates hypoxemia by reducing the alveolar PCO_2 . This was associated with an increasing number of visually scored PB cycles and as well with a significant rise in cardiorespiratory measures of PB extracted through signal processing (Table 3). Therefore, the characterization of cardiorespiratory dynamics is useful to detect physiologic effects of acclimatization. The increase in measures of PB observed with acclimatization despite a simultaneous increase in oxygen saturation is consistent with an ongoing increase in ventilatory sensitivity to hypoxia and carbon dioxide during prolonged exposure to extreme altitude [32]. Consequently, the robust automatic quantification of PBI, proposed in this study, provides a new approach to assess physiologic changes to adaptation in high altitude beyond the current analysis.

A particular and unique strength of our study is the application of time–frequency signal processing and visual analysis to the same data obtained unobtrusively during challenging field conditions in a large sample of subjects. Thus, the different approaches could be directly compared.

5 Conclusions

The results of the current study demonstrate that the proposed time-varying signal processing techniques applied to ventilation and heart rate are suitable to provide objective information about the cardiorespiratory pattern permitting to identify and quantify periodic breathing in an automatic approach. Employing a time-varying analysis allowed the detection of alterations in cardiorespiratory oscillations over the course of changes in altitude, physical activity and acclimatization. Therefore, the time-varying signal processing techniques seem to be valuable tools for the investigation of the respiratory and cardiac response to various environmental stimuli and diseases. Accordingly, in this study the automatic characterization of cardiorespiratory dynamics has shown that PB increases as climbers acclimatize during ascent to extreme altitude.

Acknowledgments This work was supported by an international cooperation Grant of the Swiss National Science Foundation (SNSF), a mobility grant of the CIBER de Bioingeniería, Biomateriales y Nanomedicina (CIBER-BBN) and by the Ministerio de Economía y Competitividad from Spanish Government under Grant TEC2010-21703-C03-01, and by Grants from the Lung Lige of Zurich, Switzerland.

Appendix: Methods used for time series analysis

Power spectral density

The signal $x(n)$ is modeled through an autoregressive model by

$$x(n) = - \sum_{k=1}^p a[k] \cdot x(n - k) + e(n)$$

where $e(n)$ denotes zero-mean white noise with variance σ_e^2 , $a[k]$ the AR coefficients and p the model order. Once the autoregressive coefficients and the variance σ_e^2 have been estimated, the PSD of an autoregressive process is computed by means of

$$\hat{P}_{xAR}(f) = \frac{\sigma_e^2}{|1 + \sum_{k=1}^p a[k] \cdot e^{-j2\pi f k T}|^2}$$

being T the sampling period.

The advantage of model-based frequency estimation is its capacity to predict future samples outside of the observation interval, instead of assuming zero as occurs with conventional nonparametric or Fourier-based spectral analysis [34]. The accuracy of the AR model was evaluated through the mean square prediction error. The optimum model order (ranging from 2 to 50) was selected for each signal according to the criterion proposed by Rissanen [30], based on selecting the model order that minimizes the description length.

Coherence

The coherence function measures the strength of the linear interaction between two time series at each frequency. Its value ranges from 0, implying no temporal correlation between the two signals to 1 implying maximum correlation. It is described as

$$C_{xy}(f) = \frac{|P_{xy}(f)|}{\sqrt{P_x(f) \cdot P_y(f)}}$$

where $P_x(f)$ and $P_y(f)$ are the PSD of both signals $x(n)$ and $y(n)$, respectively, and $P_{xy}(f)$ is the cross-PSD between them. In order to get higher frequency resolution, a parametric coherence is implemented in this study [19].

In parametric coherence analysis, a bivariate autoregressive model is applied to calculate the parametric cross-PSD. The relationship between both signals is described by

$$\mathbf{S}(n) = - \sum_{k=1}^p \mathbf{A}[k] \mathbf{S}(n - k) + \mathbf{E}(n)$$

where the matrix **S** contains both signals, matrix **A** autoregressive coefficients and matrix **E** zero-mean white noise inputs.

$$\begin{bmatrix} x(n) \\ y(n) \end{bmatrix} = \sum_{k=1}^p \begin{bmatrix} a_{xx}(k) & a_{xy}(k) \\ a_{yx}(k) & a_{yy}(k) \end{bmatrix} \cdot \begin{bmatrix} x(n-k) \\ y(n-k) \end{bmatrix} + \begin{bmatrix} e_x(n) \\ e_y(n) \end{bmatrix}$$

The matrix of PSD for this bivariate autoregressive model is obtained by

$$P(f) = \begin{bmatrix} P_{xx} & P_{xy} \\ P_{yx} & P_{yy} \end{bmatrix} = A(f) \begin{bmatrix} \sigma_{xx}^2 & \sigma_{xy}^2 \\ \sigma_{yx}^2 & \sigma_{yy}^2 \end{bmatrix} A^*(f)$$

where * denotes the conjugate transpose of the matrix. The matrix **A** is obtained through

$$A(f) = I + \sum_{k=1}^p A[k] \cdot e^{-j2\pi f k T}$$

Complexity analysis

Approximate entropy (ApEn) and sample entropy (SampEn) provide quantitative information about the complexity of the signals. ApEn is approximately equal to the negative average natural logarithm of the conditional probability that two sequences that are similar for *m* points remain similar, that is, within a tolerance *r*, at the next point. In order to avoid the occurrence of *ln(0)* in the calculations, ApEn algorithm counts each sequence as matching itself. ApEn is therefore heavily dependent on the record length and lacks relative consistency. SampEn is the negative natural logarithm of the conditional probability that two sequences similar for *m* points remain similar at the next point, where self-matches are not included in calculating the probability [8].

Considering the signal *x(n)* and the parameters *m* and *r*, the ApEn is computed by

1. Form the *m*-vectors

$$X(i) = [x(i), x(i+1), \dots, x(i+m-1)]; \quad 1 \leq i \leq N-m+1$$

being *N* the length of the signal.

2. Calculate distances between vectors

$$d[X(i), X(j)] = \max_{k=1, \dots, m} (|x(i+k) - x(j+k)|)$$

3. Compute frequency or regularity of similar patterns

$$C_r^m(i) = \frac{N^m(i)}{N-m+1}$$

where *N^m(i)* is the number of *j* ($1 \leq j \leq N-m+1$) so that $d[X(i), X(j)] \leq r$.

4. Take the natural logarithm of each *C_r^m* and average it over

$$\varnothing^m(r) = \frac{1}{N-m+1} \sum_{i=1}^{N-m+1} \ln(C_r^m(i))$$

5. Repeat this process for *m + 1* and the ApEn is finally computed as follows

$$ApEn(m, r, N) = \varnothing^m(r) - \varnothing^{m+1}(r)$$

Considering the signal *x(n)* and the parameters *m* and *r*, the SampEn is computed by

1. Form the *m*-vectors

$$X(i) = [x(i), x(i+1), \dots, x(i+m-1)]; \quad 1 \leq i \leq N-m+1$$

being *N* the length of the signal.

2. Calculate distances between vectors

$$d[X(i), X(j)] = \max_{k=1, \dots, m} (|x(i+k) - x(j+k)|)$$

3. Define for each of *i* ($1 \leq i \leq N-m$)

$$B_i^m(r) = \frac{N^m(i)}{N-m+1}$$

$$A_i^m(r) = \frac{N^{m+1}(i)}{N-m+1}$$

where *N^m(i)* is the number of *j* ($1 \leq j \leq N-m+1$), $j \neq i$ so that $d[X(i), X(j)]_m \leq r$, and *N^{m+1}(i)* is the number of *j* ($1 \leq j \leq N-m+1$), $j \neq i$ so that $d[X(i), X(j)]_{m+1} \leq r$.

4. Compute

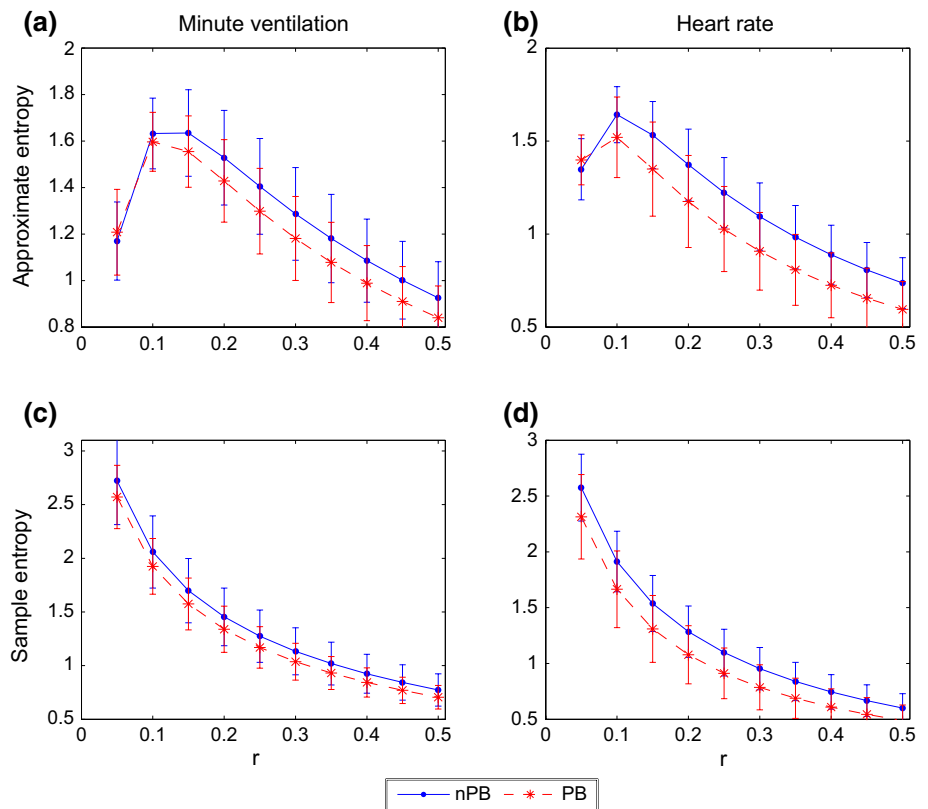
$$B^m(r) = \frac{1}{N-m} \sum_{i=1}^{N-m} B_i^m(r)$$

$$A^m(r) = \frac{1}{N-m} \sum_{i=1}^{N-m} A_i^m(r)$$

5. SampEn is finally computed as follows

$$SampEn(m, r, N) = -\ln(A^m(r)/B^m(r))$$

Fig. 7 Approximate entropy (a, b) and Sample entropy (c, d) of V_E and HR for periods with and without PB (PB and nPB, respectively) with different tolerance (r) values, being $m = 2$. Dotted and solid lines represent PB and nPB periods, respectively



The complexity of the V_E and HR signals was evaluated with tolerance values ranging from 0.05 to 0.5 and $m = 2$ (see Fig. 7). Sample entropy and approximate entropy of V_E and HR for PB and nPB periods with different tolerance values are plotted. According to this analysis and previous studies, the tolerance value of 0.15 was selected for further processing [2].

References

1. Bloch KE, Barandun J, Sackner MA (1995) Effect of mouth-piece breathing on cardiorespiratory response to intense exercise. *Am J Respir Crit Care Med* 151:1087–1092
2. Bloch K, Myers J, Senn O (2006) Sample entropy as a metric to quantify periodic breathing during high altitude climbing. *Eur Respir J* 28(suppl):195s
3. Bloch KE, Turk AJ, Maggiorini M et al (2009) Effect of ascent protocol on acute mountain sickness and success at Muztagh Ata, 7546 m. *High Alt Med Biol* 10:25–32
4. Bloch KE, Latshang TD, Turk AJ et al (2010) Nocturnal periodic breathing during acclimatization at very high altitude at Mount Muztagh Ata (7,546 m). *Am J Respir Crit Care Med* 182:562–568
5. Brack T (2003) Cheyne-Stokes respiration in patients with congestive heart failure. *Swiss Med Wkly* 133:605–610
6. Brack T, Thüer I, Clarenbach CFC et al (2007) Daytime Cheyne-Stokes respiration in ambulatory patients with severe congestive heart failure is associated with increased mortality. *Chest* 132:1463–1471
7. Brüllmann G, Thurnheer R, Bloch E et al (2010) Respiratory monitoring by inductive plethysmography in unrestrained subjects using position sensor-adjusted calibration. *Respiration* 79:112–120
8. Chen X, Solomon I, Chon K (2005) Comparison of the use of approximate entropy and sample entropy: applications to neural respiratory signal. *Proc IEEE Conf Eng Med Biol* 4:4212–4215
9. Clarenbach CF, Senn O, Bloch KE (2003) A portable inductance plethysmograph for monitoring ventilation in unrestrained subjects. *Eur Respir J* 22:408s
10. Dempsey JA (2005) Crossing the apnoeic threshold: causes and consequences. *Exp Physiol* 90:13–24
11. Dempsey JA, Veasey SC, Morgan BJ, O'Donnell CP (2010) Pathophysiology of sleep apnea. *Physiol Rev* 90:47–112
12. Fowler AC (2003) Periodic breathing at high altitude. *J Math Appl Med Biol* 19:293–313
13. Gallagher S, Hackett PH (2004) High-altitude illness. *Emerg Med Clin N Am* 22:329–355, viii
14. Garde A, Giraldo BF, Jané R, Sornmo L (2009) Time-varying respiratory pattern characterization in chronic heart failure patients and healthy subjects. *Proc. IEEE Conf. Eng. Med. Biol. Minneapolis, Minnesota, USA*, pp 4007–4010
15. Garde A, Sörnmo L, Jané R, Giraldo BF (2010) Breathing pattern characterization in chronic heart failure patients using the respiratory flow signal. *Ann Biomed Eng* 38:3572–3580
16. Garde A, Sörnmo L, Jané R, Giraldo BF (2010) Correntropy-based spectral characterization of respiratory patterns in patients with chronic heart failure. *IEEE Trans Biomed Eng* 57:1964–1972
17. Garde A, Sornmo L, Jane R, Giraldo BF (2010) Correntropy-based nonlinearity test applied to patients with chronic heart failure. *Proc IEEE Conf Eng Med Biol* 2010:2399–2402

18. Garde A, Giraldo BF, Jane R et al (2012) Periodic breathing during ascent to extreme altitude quantified by spectral analysis of the respiratory volume signal. *Proc IEEE Conf Eng Med Biol* 2012:707–710
19. Indic P, Bloch-Salisbury E, Bednarek F et al (2011) Assessment of cardio-respiratory interactions in preterm infants by bivariate autoregressive modeling and surrogate data analysis. *Early Hum Dev* 87:477–487
20. Khoo MC, Kronauer RE, Strohl KP, Slutsky AS (1982) Factors inducing periodic breathing in humans: a general model. *J Appl Physiol* 53:644–659
21. Kohler M, Kriemler S, Wilhelm EM et al (2008) Children at high altitude have less nocturnal periodic breathing than adults. *Eur Respir J* 32:189–197
22. Latshang TD, Turk J, Hess T et al (2013) Acclimatization improves submaximal exercise economy at 5533 m. *Scand J Med Sci Sports* 23(4):458–467
23. Latshang TD, Cascio CM, Lo Grimm M et al (2013) Are nocturnal breathing, sleep and cognitive performance impaired at moderate altitude (1630–2590 m)? *Sleep* 36:1969–1976
24. Lipsitz LA, Hashimoto F, Lubowsky LP et al (1995) Heart rate and respiratory rhythm dynamics on ascent to high altitude. *Br Heart J* 74:390–396
25. Malik M, Bigger JT, Camm AJ et al (1996) Heart rate variability. Standards of measurement, physiological interpretation, and clinical use. Task Force of the European Society of Cardiology and the North American Society of Pacing and Electrophysiology. *Eur Hear J* 17:354–381
26. Mortara A, Sleight P, Pinna GD et al (1997) Abnormal awake respiratory patterns are common in chronic heart failure and may prevent evaluation of autonomic tone by measures of heart rate variability. *Circulation* 96:246–252
27. Nussbaumer-Ochsner Y, Schuepfer N, Siebenmann C, Maggiorini MBK (2011) High altitude sleep disturbances monitored by actigraphy and polysomnography. *High Alt Med Biol* 12(3):229–236
28. Nussbaumer-Ochsner Y, Ursprung J, Siebenmann C et al (2012) Effect of short-term acclimatization to high altitude on sleep and nocturnal breathing. *Sleep* 35:419–423
29. Pincus SM, Goldberger AL (1994) Physiological time-series analysis: what does regularity quantify? *Am J Physiol Hear Circ Physiol* 266:H1643–H1656
30. Rissanen J (1978) Modeling by shortest data description. *Automatica* 14:465–471
31. Sackner MA, Watson H, Belsito AS et al (1989) Calibration of respiratory inductive plethysmograph during natural breathing. *J Appl Physiol* 66:410–420
32. San T, Polat S, Cingi C et al (2013) Effects of high altitude on sleep and respiratory system and their adaptations. *Sci World J* 2013:241569. doi:10.1155/2013/241569
33. Sleep Medicine Task Force AA (1999) Sleep-related breathing disorders in adults: recommendations for syndrome definition and measurement techniques in clinical research. *Sleep* 22:667–689
34. Sörnmo L, Laguna P (2005) Bioelectrical signal processing in cardiac and neurological applications. Elsevier/Academic Press, Amsterdam
35. Szollosi I, Krum H, Kaye D, Naughton MT (2007) Sleep apnea in heart failure increases heart rate variability and sympathetic dominance. *Sleep* 11:1509–1514
36. White LB, Boashash B (1990) Cross spectral analysis of nonstationary processes. *IEEE Trans Inf Theory* 36:830–835
37. Wolf MB, Garner RP (2009) Disequilibrium between alveolar and end-pulmonary-capillary O₂ tension in altitude hypoxia and respiratory disease: an update of a mathematical model of human respiration at altitude. *Ann Biomed Eng* 37:1818–1826
38. Nussbaumer-Ochsner Y, Bloch KE (2014) Sleep. In: Swenson ER, Bärtsch P (eds) High altitude. Human adaptation to hypoxia. Springer, New York, pp 325–335